

This article has been accepted for publication in IEEE Transactions on Signal and Information Processing over Networks. This is the author's version which has not been fully edited and content may change prior to final publication. Citation information: DOI 10.1109/TSIPN.2023.3264993.

arXiv:2209.06385v3 [eess.SP] 19 Apr 2023

Spline-Like Wavelet Filterbanks with Perfect Reconstruction on Arbitrary Graphs

Junxia You and Lihua Yang

Abstract—In this work, we propose a class of spline-like wavelet filterbanks for graph signals. These filterbanks possess the properties of critical sampling and perfect reconstruction. The analysis filters are localized in the graph domain because they are polynomials in the normalized adjacency matrix of the graph. We generalize the spline-like filters in the literature so that the lowpass filter and the highpass filter can respectively remove the s highest frequency components and the r lowest frequency components of the signal, where r and s are hyperparameters specified by the users. Optimization models are formulated for the analysis filters to approximate the desired responses. Experimental results demonstrate the good locality and denoising ability of the proposed filterbanks.

Index Terms—Graph signal processing, graph wavelet filterbank, spline-like filters

I. INTRODUCTION

In recent years, complex data analysis is widely concerned. In many applications, data structures such as social networks, sensor networks and biological networks can be modelled as graphs, and the data residing on these graphs are called graph signals. With the rise of big data science, theoretical and applied research on graph signal processing (GSP) becomes increasingly important. Researchers are working to extend the theory and methods in classical signal processing to GSP. Theories about graph Fourier transform, graph filters, graph wavelets and Multiresolution analysis (MRA) on graph signals are developed [22], [27], [8], [23]. In terms of application, GSP methods are also widely used in such as point clouds analysis [12], [14], deep neural networks and computer vision [15]. However, due to the irregularity of graph structure, there are still many challenges in this field.

Wavelet analysis of graph signals is an important topic in GSP. Researchers have developed different types of graph wavelets. In [5], Crovella and Kolaczyk constructed a series of compactly supported simple functions on each neighbourhood of every vertex as graph wavelet functions. Coifman and Maggioni proposed the concept of diffusion wavelets in [4]. Gavish et al. [8] first constructed multiscale wavelet-like orthonormal

bases on hierarchical trees. Hammond et al. [11] constructed wavelet transforms in the graph domain based on the spectral graph theory. In follow-up work, they designed an almost tight wavelet frame based on the polynomial filters [26]. In [23], Shuman et al. proposed a modular framework—a multiscale pyramid transform for graph signals. All these wavelets are not critically sampled, the output has more components than the input signal, which leads to the waste of space for storing redundant information. Critically sampled wavelet filterbanks have also been proposed in many works. Narang and Ortega developed the two channel filterbanks composed of graph quadrature mirror filters and the compact support biorthogonal filterbanks in [20], [18]. Ekambaram et al. proposed the spline-like filterbanks in [7]. The exponential spline filterbanks on circulant graphs are proposed by Kotzagiannidis and Dragotti in [13], and the modified spline filterbanks are proposed by Miraki et al. in [16] and [17]. Especially, the scheme proposed in [17] utilizes the spectral domain sampling method proposed in [25].

The classical wavelets can capture local information of signals in the time domain, i.e., each sample of the transformed signal is computed by using the samples from a small neighbourhood of the original signal. This property enables wavelets to capture the details of the signal. Thus, we are interested in the spline-like filterbanks proposed in [7], since the analysis filters are polynomials in the normalized adjacency matrix of the graph, which leads to the locality of filters in the graph domain.

The authors of [7] provide results on the perfect reconstruction property of their proposed spline-like filterbanks, and formulate optimization models to obtain the desired filter responses. The filterbanks have the advantage of critical sampling, and the analysis filters are well localized in the graph domain. However, the lowpass filter they designed cannot remove the highest frequency component of the signal unless it is a degree-1 polynomial in the normalized adjacency matrix and the graph is bipartite, as discussed later in Section II-C. This will impair the denoising ability of the filterbanks. Therefore, we extend their work to enable the filterbanks with better denoising capability. The novelty and main contributions of this paper are summarized as follows.

We propose a class of spline-like filterbanks in which the lowpass (highpass) filter can remove more than one high-frequency (low-frequency) components of the signals. A perfect reconstruction theorem is established where the sampling pattern is required to meet some mild conditions and an algorithm is proposed to obtain the effective sampling pattern. Similarly, optimization problems are formulated for the anal-

This is supported by National Natural Science Foundation of China (No. 12171488) and Guangdong Province Key Laboratory of Computational Science at the Sun Yat-sen University (2020B1212060032). Note: Codes for this paper are available at <https://github.com/ConquerBroccoli/matlabcodes/tree/codes-for-thesis>. Please contact Junxia You for further questions about the codes.

Junxia You is with School of Mathematics, Sun Yat-sen University, Guangzhou, China (e-mail: youjx3@mail2.sysu.edu.cn).

Lihua Yang is with School of Mathematics, Sun Yat-sen University, Guangzhou, China and Guangdong Province Key Laboratory of Computational Science (e-mail: mcsylh@mail.sysu.edu.cn). He is the corresponding author.

ysis filters to approximate the desired frequency responses. We also construct filterbanks based on the non-normalized adjacency matrices, which is useful in some applications that require the highpass filter to eliminate the direct current (DC) signal. Besides, through a counterexample we point out a small flaw in the perfect reconstruction theorem in [7] and give a correction.

This paper is organized as follows: in Section II, we introduce some basic concepts related to the graph filterbanks and introduce the design in [7] to motivate our work. In Section III, we describe the proposed generalized spline-like filterbanks, and provide sufficient conditions for the filterbanks to be perfectly reconstructed. Besides, we give an algorithm to obtain sampling patterns that satisfy the perfect reconstruction conditions and formulate optimization models for the filters to approximate desired responses. In Section IV, experiments are conducted to demonstrate the effectiveness of the proposed filterbanks compared to the related work. Finally, we make a conclusion and discuss the limitation and future work in Section V.

II. PRELIMINARY

A. Notations

We use bold letters for matrices and vectors, calligraphic capital letters for sets, and normal letters for scalars.

The i -th entry of a vector \mathbf{x} is denoted by x_i or $\mathbf{x}(i)$. The (i, j) -th entry of a matrix \mathbf{A} is denoted by $\mathbf{A}(i, j)$. Assume that $\mathcal{I}_1, \mathcal{I}_2$ are two subsets of $\{1, \dots, N\}$, then $\mathbf{A}(\mathcal{I}_1, \mathcal{I}_2)$ denotes the submatrix consisting of entries of \mathbf{A} whose row indices are in \mathcal{I}_1 and column indices are in \mathcal{I}_2 . Let \mathbf{I}_N represent the identity matrix of order N and $\mathbf{1}, \mathbf{0}$ respectively represent the all-ones vector and the null vector whose sizes can be seen from the context.

The superscript \top denotes transposition. $\text{diag}(\cdot)$ maps a vector to a diagonal matrix, or a matrix to its main diagonal vector. The infinity norm and 2-norm of a vector $\mathbf{x} \in \mathbb{R}^N$ are defined as $\|\mathbf{x}\|_\infty = \max_{1 \leq i \leq N} |x_i|$ and $\|\mathbf{x}\|_2 = (\sum_{i=1}^N |x_i|^2)^{\frac{1}{2}}$, respectively. $\mathbf{x} > (\geq) \mathbf{0}$ means that all entries of \mathbf{x} are positive (non-negative). The 2-norm of a matrix, denoted by $\|\mathbf{A}\|_2$, is defined as the largest singular value of \mathbf{A} . The cardinality of a set \mathcal{V} is written as $|\mathcal{V}|$.

B. Graph and Graph Fourier Transform

A graph can be denoted as $\mathcal{G} = (\mathcal{V}, \mathcal{E}, \mathbf{A})$ with vertex set $\mathcal{V} = \{1, \dots, N\}$, edge set $\mathcal{E} = \{(i, j) \mid i \sim j\}$ and adjacency matrix \mathbf{A} , where $i \sim j$ means that vertices i and j are connected. We only consider connected, undirected and weighted graphs without self-loops or multiple edges in this paper. The elements of \mathbf{A} indicate the adjacency relationship of pairs of vertices such that $\mathbf{A}(i, j) > 0$ if $(i, j) \in \mathcal{E}$ and $\mathbf{A}(i, j) = 0$ otherwise. Let $\mathbf{D} = \text{diag}(d_1, \dots, d_N)$ denote the degree matrix of \mathbf{A} , where $d_i = \sum_{j=1}^N \mathbf{A}(i, j)$ is the degree of vertex i .

Due to the connectivity of \mathcal{G} , \mathbf{D} is non-singular. Thus, we can define the symmetric normalized adjacency matrix as $\mathbf{A}^S = \mathbf{D}^{-\frac{1}{2}} \mathbf{A} \mathbf{D}^{-\frac{1}{2}}$. Correspondingly, the symmetric normalized Laplacian matrix of \mathcal{G} is defined as $\mathbf{L}^S = \mathbf{I}_N - \mathbf{A}^S$

[3]. Since \mathbf{L}^S is real symmetric and positive semi-definite, there exists a set of orthonormal eigenvectors $\{\mathbf{u}_i\}_{i=1}^N$ and real eigenvalues $0 = \lambda_1 < \lambda_2 \leq \dots \leq \lambda_N$ such that $\mathbf{L}^S = \mathbf{U} \mathbf{\Lambda} \mathbf{U}^\top$, where $\mathbf{U} = (\mathbf{u}_1, \dots, \mathbf{u}_N)$ and $\mathbf{\Lambda} = \text{diag}(\lambda_1, \dots, \lambda_N)$. Obviously, the eigendecomposition of \mathbf{A}^S can be written as $\mathbf{A}^S = \mathbf{U} \text{diag}(\xi_1, \dots, \xi_N) \mathbf{U}^\top$ with $\xi_i = 1 - \lambda_i$. In the rest of the paper, $\{\mathbf{u}_i\}_{i=1}^N$ and \mathbf{U} will always denote the eigenvectors and the corresponding eigenmatrix of \mathbf{L}^S , and \mathbf{u}_i is called the i -th **Fourier basis vector** of frequency λ_i which increases as i goes from 1 to N .

A graph signal $x : \mathcal{V} \rightarrow \mathbb{R}$ is a function defined on the vertices of the graph. If the labels of the vertices are fixed, the signal can also be written as a vector $\mathbf{x} \in \mathbb{R}^N$. In this paper, we define the graph Fourier transform (GFT) of signal \mathbf{x} as $\hat{\mathbf{x}} = \mathbf{U}^\top \mathbf{x}$ [24]. Thus, \mathbf{x} can be represented as $\mathbf{x} = \sum_{l=1}^N \hat{\mathbf{x}}(l) \mathbf{u}_l$, and $\hat{\mathbf{x}}(l) \mathbf{u}_l$ is referred to as the component of \mathbf{x} with frequency λ_l .

C. Two-Channel Filterbanks and Related Work

A two-channel filterbank is shown in Figure 1. It is a collection of filters and samplers. The filters $\mathbf{H}_L, \mathbf{H}_H$ are called analysis filters and the filter \mathbf{H}_{INV} is called synthesis filter, where the subscript L represents lowpass (LP) and H represents highpass (HP). The downsampler and the upsampler are denoted by \downarrow and \uparrow respectively.

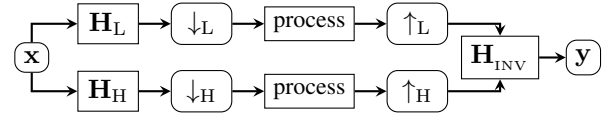


Fig. 1. A two-channel filterbank.

Given a graph signal $\mathbf{x} \in \mathbb{R}^N$, the analysis filters $\mathbf{H}_L, \mathbf{H}_H$ attenuate the high and low frequency components of \mathbf{x} respectively. After that, the filtered signal in each channel will be downsampled to produce signals $\mathbf{y}_L = (\downarrow_L) \mathbf{H}_L \mathbf{x}$ and $\mathbf{y}_H = (\downarrow_H) \mathbf{H}_H \mathbf{x}$. If the sum of lengths of \mathbf{y}_L and \mathbf{y}_H equals N , the filterbank is said to be critically sampled. In this case, we can define a sampling matrix $\mathbf{K} = \text{diag}(k_1, \dots, k_N)$ with $k_i \in \{1, -1\}, \forall i = 1, \dots, N$ such that \mathbf{y}_L is a subvector of $\mathbf{H}_L \mathbf{x}$ with indices in $\{i \mid k_i = 1\}$ and \mathbf{y}_H is a subvector of $\mathbf{H}_H \mathbf{x}$ with indices in $\{i \mid k_i = -1\}$.

After downsampling, the signals may be encoded for transmission or storage, which may result in loss of information. To construct a perfect reconstruction filterbank such that $\mathbf{y} = \mathbf{x}$, we omit the processing stage, i.e., upsample the signals immediately after downsampling. Thus, we have

$$\mathbf{y} = \mathbf{H}_{\text{INV}} \left[\frac{1}{2} (\mathbf{I}_N + \mathbf{K}) \mathbf{H}_L + \frac{1}{2} (\mathbf{I}_N - \mathbf{K}) \mathbf{H}_H \right] \mathbf{x}. \quad (1)$$

The filterbank is perfectly reconstructed if and only if (iff)

$$\mathbf{H}_{\text{INV}} \left[\frac{1}{2} (\mathbf{I}_N + \mathbf{K}) \mathbf{H}_L + \frac{1}{2} (\mathbf{I}_N - \mathbf{K}) \mathbf{H}_H \right] = \mathbf{I}_N. \quad (2)$$

Inspired by the classical first-order spline filters, the authors of [7] designed a class of spline-like analysis filters for the two-channel filterbanks on graphs, which are

$$\begin{aligned}\mathbf{H}_L^S &= \frac{1}{2} \left(\mathbf{I}_N + \sum_{l=1}^J w_l (\mathbf{A}^S)^l \right), \\ \mathbf{H}_H^S &= \frac{1}{2} \left(\mathbf{I}_N - \sum_{l=1}^J w_l (\mathbf{A}^S)^l \right),\end{aligned}\quad (3)$$

where the weights w_1, \dots, w_J are positive scalars. The corresponding filter responses are given as

$$\begin{aligned}\mathbf{h}_L^S(i) &= \frac{1}{2} \left(1 + \sum_{l=1}^J w_l \xi_i^l \right), \\ \mathbf{h}_H^S(i) &= \frac{1}{2} \left(1 - \sum_{l=1}^J w_l \xi_i^l \right),\end{aligned}\quad i = 1, \dots, N. \quad (4)$$

The weights give us the flexibility to optimize the filter responses to the desired responses. Degree J is a hyperparameter to be specified. The smaller J is, the better the locality of filters in the graph domain (vertex domain). Let us take an example to illustrate the locality of filters in the graph domain. When $J = 1$, we have

$$(\mathbf{H}_L^S \mathbf{x})(i) = \frac{1}{2} \left(x_i + w_1 \sum_{\mathbf{A}^S(i,j) > 0} x_j \mathbf{A}^S(i,j) \right). \quad (5)$$

It is clear that $(\mathbf{H}_L^S \mathbf{x})(i)$ is determined by the entries of \mathbf{x} located on the one-hop neighbourhood of vertex i . A k -hop neighbourhood of vertex i is defined as $\{j \mid [\sum_{l=1}^k (\mathbf{A}^S)^l](i,j) > 0\}$.

The authors of [7] provided sufficient conditions for perfect reconstruction of the filterbanks with analysis filters defined in (3).

Theorem 1. [7] *For any connected graph, the spline filters defined in (3) form a critically-sampled, perfect reconstruction filterbank for any downsampling pattern, as long as the weights satisfy one of the following properties:*

$$\left\{ \begin{array}{l} w_l > 0, \quad l = 1, \dots, J, \\ \sum_{l=1}^J w_l = 1, \end{array} \right. \quad \text{or} \quad \left| \sum_{l=1}^J w_l \xi_i^l \right| > 1, \quad (6)$$

for any $i = 1, \dots, N$, where $\{\xi_i\}_{i=1}^N$ are the eigenvalues of \mathbf{A}^S .

We point out that the theorem is not mathematically accurate in the extreme case where $J = 1$ and $\mathbf{K} = \mathbf{I}_N$, i.e., the downsampling pattern does not retain any highpass components. A counterexample is given below. When $J = 1$, there holds $w_1 = 1$ and thus $\mathbf{H}_L^S = \frac{1}{2}(\mathbf{I}_N + \mathbf{A}^S)$. If -1 is an eigenvalue of \mathbf{A}^S (i.e., the graph is bipartite [2]), then 0 is an eigenvalue of \mathbf{H}_L^S . In this case,

$$\frac{1}{2}(\mathbf{I}_N + \mathbf{K})\mathbf{H}_L^S + \frac{1}{2}(\mathbf{I}_N - \mathbf{K})\mathbf{H}_H^S = \mathbf{H}_L^S, \quad (7)$$

and \mathbf{H}_L^S is irreversible. Consequently, there is no matrix \mathbf{H}_{INV}^S satisfying the perfect reconstruction equation (2). However, the conclusion of the theorem can be proven correct if the downsampling pattern preserves at least one lowpass component and one highpass component, i.e., $\mathbf{K} \neq \pm \mathbf{I}_N$.

By Theorem 1, one can formulate an optimization model to optimize the weights w_1, \dots, w_J to obtain the desired filter responses while satisfying the conditions for perfect reconstruction. For example, a least-square formulation is as follows [7]:

$$\begin{aligned}\min_{\mathbf{w} \in \mathbb{R}^J} \quad & \|\mathbf{H}^{\text{des}} - \mathbf{H}_L^S\|_2 \\ \text{s.t.} \quad & \mathbf{w}^\top \mathbf{1}_J = 1, \\ & \mathbf{w} > 0,\end{aligned}\quad (8)$$

where $\mathbf{w} = [w_1, \dots, w_J]^\top$ and \mathbf{H}^{des} is a desired lowpass filter. Figure 6 in [7] shows an example of lowpass and highpass spline-like filter responses on the Tapir dataset, where $J = 10$ and \mathbf{H}^{des} is an ideal lowpass filter. We notice that the filter responses in the figure have a wide range from 0 to 10^{15} and the lowpass response approaches 0 near zero frequency, making it a bandpass filter instead of a lowpass filter. In addition, the presented ‘‘highpass’’ filter is not actually highpass since the filter response has high amplitude in the low frequency region and low amplitude in the high frequency region.

We find that under the first set of conditions of Theorem 1, the highpass filter \mathbf{H}_H^S has a zero response to the lowest frequency Fourier basis vector \mathbf{u}_1 (while the second set of conditions does not guarantee this), but the lowpass filter \mathbf{H}_L^S has a non-zero response to \mathbf{u}_N , the highest frequency Fourier basis vector, unless $J = 1$ and the graph is bipartite. This is because under the first set of conditions, the LP filter response $\mathbf{h}_L^S(i) = 0$ iff $\sum_{l=1}^J w_l \xi_i^l = -1$, which can only be achieved when $J = 1$ and $\xi_i = -1$. However, there exists an eigenvalue $\xi_i = -1$ iff the graph is bipartite. This fact weakens the denoising ability of the analysis filters for non-bipartite graphs. In Section III, we improve their design so that the LP filter has zero responses to the s Fourier basis vectors $\{\mathbf{u}_i\}_{i=N-s+1}^N$ with the highest frequencies and the HP filter has zero responses to the r Fourier basis vectors $\{\mathbf{u}_i\}_{i=1}^r$ with the lowest frequencies, where $r, s \geq 1$ are hyperparameters specified by the users.

III. GENERALIZATION

A. Main Theorem

Hereafter, we consider analysis filters of the form:

$$\left\{ \begin{array}{l} \mathbf{H}_L = \frac{1}{2}(\mathbf{I}_N + \sum_{l=1}^J w_l (\mathbf{A}^S)^{l-1}) \\ \mathbf{H}_H = \frac{1}{2}(\mathbf{I}_N - \sum_{l=1}^J w_l (\mathbf{A}^S)^{l-1}) \end{array} \right., \quad (9)$$

where $\mathbf{w} = [w_1, \dots, w_J]^\top \in \mathbb{R}^J$ and $J \geq 2$. Recall that $\mathbf{A}^S = \mathbf{U} \text{diag}(\xi_1, \dots, \xi_N) \mathbf{U}^\top$. For simplicity, denote

$$\mathbf{G} = \sum_{l=1}^J w_l (\mathbf{A}^S)^{l-1}, \quad \gamma_i = \sum_{l=1}^J w_l \xi_i^{l-1},$$

$$\mathbf{\Gamma} = \text{diag}(\gamma_1, \dots, \gamma_N).$$

Then $\mathbf{G} = \mathbf{U} \mathbf{\Gamma} \mathbf{U}^\top$. Similar to the scheme proposed in [7], we will optimize the weights \mathbf{w} for the desired filter responses while maintaining the perfect reconstruction property of the filterbank.

There are some discussions before giving the formulation. Given a sampling matrix \mathbf{K} and analysis filters $\mathbf{H}_L, \mathbf{H}_H$, the filterbank is perfectly reconstructed iff the synthesis filter \mathbf{H}_{INV} exists such that (2) holds. A simple calculation shows that

$$\frac{1}{2}(\mathbf{I}_N + \mathbf{K})\mathbf{H}_L + \frac{1}{2}(\mathbf{I}_N - \mathbf{K})\mathbf{H}_H = \frac{1}{2}(\mathbf{I}_N + \mathbf{K}\mathbf{G}). \quad (10)$$

Thus, \mathbf{H}_{INV} exists iff $\mathbf{I}_N + \mathbf{K}\mathbf{G}$ is invertible, in which case $\mathbf{H}_{\text{INV}} = 2(\mathbf{I}_N + \mathbf{K}\mathbf{G})^{-1}$. Next, we will design \mathbf{K} and \mathbf{G} so that the following two conditions are satisfied:

- (1°) $\mathbf{I}_N + \mathbf{K}\mathbf{G}$ is invertible;
 (2°) $\mathbf{H}_L \mathbf{u}_i = \mathbf{0}, i = N - s + 1, \dots, N$ and $\mathbf{H}_H \mathbf{u}_i = \mathbf{0}, i = 1, \dots, r$, where $r \geq 1, s \geq 1$ are hyperparameters.

Since $\mathbf{G} = \mathbf{U}\mathbf{T}\mathbf{U}^\top$, we actually need to determine \mathbf{T} and \mathbf{K} . The entire process is as follows: first, we provide Theorem 2 which states the sufficient conditions for \mathbf{T} and \mathbf{K} to satisfy (1°) and (2°). Second, according to the theorem, we formulate optimization models in Section III-B to compute the weights \mathbf{w} , which determines \mathbf{T} , and provide an algorithm in Section III-C to partition the vertex set \mathcal{V} into two disjoint subsets $\{\mathcal{A}, \mathcal{B}\}$, which gives \mathbf{K} . The process of constructing the proposed filterbank is shown in Figure 2.

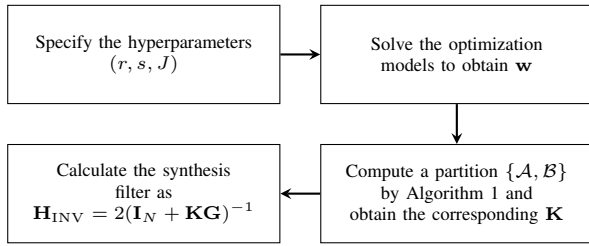


Fig. 2. The diagram of the whole process of constructing the proposed filterbank.

In the following, let $\mathcal{I}_r = \{1, \dots, r\}$, $\mathcal{I}_s = \{N+1-s, \dots, N\}$. $\mathbf{U}(\mathcal{A}, \mathcal{I}_r)$ denotes the submatrix consisting of entries of \mathbf{U} with row indices in \mathcal{A} and column indices in \mathcal{I}_r . $\mathbf{U}(\mathcal{B}, \mathcal{I}_s)$ has a similar meaning.

Theorem 2. Given $r \geq 1, s \geq 1$ satisfying $r+s \leq N$. Assume that the eigenvalues of \mathbf{G} satisfy

$$\gamma_1 = \dots = \gamma_r = 1, \quad \gamma_{N+1-s} = \dots = \gamma_N = -1 \quad (11)$$

and one of the following two sets of conditions:

$$\begin{aligned} |\gamma_i| < 1, \quad \forall r < i < N+1-s, \\ \text{or} \\ |\gamma_i| > 1, \quad \forall r < i < N+1-s. \end{aligned} \quad (12)$$

Then

$$\begin{aligned} (\mathbf{I}_N - \mathbf{G})\mathbf{u}_i &= \mathbf{0}, \quad \forall i = 1, \dots, r, \\ (\mathbf{I}_N + \mathbf{G})\mathbf{u}_i &= \mathbf{0}, \quad \forall i = N-s+1, \dots, N. \end{aligned} \quad (13)$$

Furthermore, if the vertex set $\mathcal{V} = \{1, \dots, N\}$ can be partitioned into two disjoint subsets \mathcal{A}, \mathcal{B} such that both the submatrices $\mathbf{U}(\mathcal{A}, \mathcal{I}_r)$ and $\mathbf{U}(\mathcal{B}, \mathcal{I}_s)$ are of full column rank,

then $\mathbf{I}_N + \mathbf{K}\mathbf{G}$ is invertible, where \mathbf{K} is a diagonal matrix satisfying

$$\mathbf{K}(i, i) = \begin{cases} 1, & i \in \mathcal{A}, \\ -1, & i \in \mathcal{B}. \end{cases} \quad (14)$$

Proof. 1) By $\mathbf{G} = \mathbf{U}\mathbf{T}\mathbf{U}^\top$, it is easy to prove (13).

2) Suppose $\mathbf{x} \in \mathbb{R}^N$ lies in the null space of $\mathbf{I}_N + \mathbf{K}\mathbf{G}$, i.e., $(\mathbf{I}_N + \mathbf{K}\mathbf{U}\mathbf{T}\mathbf{U}^\top)\mathbf{x} = \mathbf{0}$. Let $\mathbf{y} = \mathbf{U}^\top \mathbf{x}$, then

$$\begin{aligned} 0 &= \|\mathbf{x}\|_2^2 - \|\mathbf{K}\mathbf{U}\mathbf{T}\mathbf{U}^\top \mathbf{x}\|_2^2 \\ &= \|\mathbf{y}\|_2^2 - \|\mathbf{T}\mathbf{y}\|_2^2 = \sum_{i=1}^N (1 - \gamma_i^2) y_i^2. \end{aligned} \quad (15)$$

The second equality holds because the orthogonal transformation preserves the 2-norm of a vector and both \mathbf{K}, \mathbf{U} are orthogonal matrices.

Since $\gamma_i^2 < 1$ or $\gamma_i^2 > 1$ for all $r < i < N+1-s$, all corresponding y_i are 0. Thus,

$$\mathbf{x} = \mathbf{U}\mathbf{y} = \sum_{i=1}^r y_i \mathbf{u}_i + \sum_{i=N+1-s}^N y_i \mathbf{u}_i, \quad (16)$$

and

$$\mathbf{G}\mathbf{x} = \mathbf{U}\mathbf{T}\mathbf{y} = \sum_{i=1}^r y_i \mathbf{u}_i - \sum_{i=N+1-s}^N y_i \mathbf{u}_i. \quad (17)$$

Denote $\mathbf{x}_1 = \sum_{i=1}^r y_i \mathbf{u}_i$ and $\mathbf{x}_{-1} = \sum_{i=N+1-s}^N y_i \mathbf{u}_i$. Combining (16) and (17) with $(\mathbf{I}_N + \mathbf{K}\mathbf{G})\mathbf{x} = \mathbf{0}$ gives

$$\mathbf{x}_1 + \mathbf{x}_{-1} + \mathbf{K}\mathbf{x}_1 - \mathbf{K}\mathbf{x}_{-1} = \mathbf{0}. \quad (18)$$

Premultiplying \mathbf{K} on both sides of (18) gives

$$\mathbf{x}_1 - \mathbf{x}_{-1} + \mathbf{K}\mathbf{x}_1 + \mathbf{K}\mathbf{x}_{-1} = \mathbf{0}. \quad (19)$$

Calculating the sum and difference of (18) and (19) shows that

$$(\mathbf{I}_N + \mathbf{K})\mathbf{x}_1 = (\mathbf{I}_N - \mathbf{K})\mathbf{x}_{-1} = \mathbf{0}. \quad (20)$$

According to the definition of \mathbf{K} , there must hold

$$\mathbf{x}_1(i) = 0, \quad \forall i \in \mathcal{A}, \quad \mathbf{x}_{-1}(i) = 0, \quad \forall i \in \mathcal{B}. \quad (21)$$

Since $\mathbf{x}_1 = \sum_{i=1}^r y_i \mathbf{u}_i$ and $\mathbf{U}(\mathcal{A}, \mathcal{I}_r)$ has full column rank, there holds $y_1 = \dots = y_r = 0$. Similarly, $y_{N+1-s} = \dots = y_N = 0$. Therefore, $\mathbf{x} = \mathbf{x}_1 + \mathbf{x}_{-1} = \mathbf{0}$, and $\mathbf{I}_N + \mathbf{K}\mathbf{G}$ is invertible. ■

Remark: Note that if both r and s are too large, there may not exist a partition $\{\mathcal{A}, \mathcal{B}\}$ of vertices such that both $\mathbf{U}(\mathcal{A}, \mathcal{I}_r)$ and $\mathbf{U}(\mathcal{B}, \mathcal{I}_s)$ are of full column rank. But in practice, we usually set r and s to be numbers much smaller than N , in which case finding such a partition is generally not difficult and even full of options.

Next, consider a special case where the intrinsic graph $\mathcal{G}_b = \{\mathcal{V}_b, \mathcal{E}_b, \mathbf{A}_b\}$ is bipartite, that is, the vertex set \mathcal{V}_b can be partitioned into two disjoint subsets \mathcal{A}, \mathcal{B} (which are called two parts of \mathcal{G}_b) such that connections exist only between \mathcal{A} and \mathcal{B} . Then a natural sampling pattern is to keep one of the two parts in the lowpass channel and the other in the highpass channel [20], [18]. We will provide sufficient conditions for

the filterbank to be perfectly reconstructed under this sampling pattern.

We first introduce some notations. Suppose \mathcal{G}_b is connected. Let \mathbf{A}_b^S be the normalized adjacency matrix of \mathcal{G}_b whose eigen-decomposition is $\mathbf{A}_b^S = \mathbf{U}_b \text{diag}(\xi_1^b, \dots, \xi_N^b) \mathbf{U}_b^\top$. The eigenvalues $\{\xi_i^b\}_{i=1}^N$ are assumed to be in **descending** order. Similarly, define $\mathbf{G}_b = \sum_{l=1}^J w_l (\mathbf{A}_b^S)^{l-1}$. It can also be written as $\mathbf{G}_b = \mathbf{U}_b \text{diag}(\gamma_1^b, \dots, \gamma_N^b) \mathbf{U}_b^\top$, where $\gamma_i^b = \sum_{l=1}^J w_l (\xi_i^b)^{l-1}$, $\forall i = 1, \dots, N$.

Proposition 3. *If $1 \leq r, s \leq \frac{1}{2} \text{rank}(\mathbf{A}_b^S)$, then both $\mathbf{U}_b(\mathcal{A}, \mathcal{I}_r)$ and $\mathbf{U}_b(\mathcal{B}, \mathcal{I}_s)$ are full column rank. Define \mathbf{K}_b as a diagonal matrix with*

$$\mathbf{K}_b(i, i) = \begin{cases} 1, & i \in \mathcal{A}, \\ -1, & i \in \mathcal{B}. \end{cases} \quad (22)$$

If the eigenvalues $\{\gamma_i^b\}_{i=1}^N$ of \mathbf{G}_b satisfy the conditions (11) and (12) in Theorem 2, then $\mathbf{I}_N + \mathbf{K}_b \mathbf{G}_b$ is invertible.

Proof. Since \mathcal{G}_b is bipartite, we can label the vertices so that

$$\mathbf{A}_b^S = \begin{pmatrix} \mathbf{0} & \mathbf{R} \\ \mathbf{R}^\top & \mathbf{0} \end{pmatrix},$$

where $\mathbf{R} \in \mathbb{R}^{|\mathcal{A}| \times |\mathcal{B}|}$. Denote \mathbf{v}_i the i -th column of \mathbf{U}_b and write \mathbf{v}_i as $\mathbf{v}_i = [\mathbf{v}_{i\mathcal{A}}^\top, \mathbf{v}_{i\mathcal{B}}^\top]^\top$, where $\mathbf{v}_{i\mathcal{A}}$ and $\mathbf{v}_{i\mathcal{B}}$ are the subvectors of \mathbf{v}_i whose indices are respectively in \mathcal{A} and \mathcal{B} .

Since \mathcal{G}_b is bipartite, it is known that if $[\mathbf{v}_{i\mathcal{A}}^\top, \mathbf{v}_{i\mathcal{B}}^\top]^\top$ is an eigenvector of \mathbf{A}_b^S associated with eigenvalue ξ_i^b , then $[\mathbf{v}_{i\mathcal{A}}^\top, -\mathbf{v}_{i\mathcal{B}}^\top]^\top$ is an eigenvector of \mathbf{A}_b^S associated with eigenvalue $-\xi_i^b$ [3]. Suppose $\{\xi_i^b\}_{i=1}^N$ has p positive terms, then it also has p negative terms. Hence, $\text{rank}(\mathbf{A}_b^S) = 2p$.

For any $1 \leq i \leq N$ satisfying $\xi_i^b \neq 0$, we have

$$\mathbf{A}_b^S \begin{bmatrix} \mathbf{v}_{i\mathcal{A}} \\ \mathbf{v}_{i\mathcal{B}} \end{bmatrix} = \xi_i^b \begin{bmatrix} \mathbf{v}_{i\mathcal{A}} \\ \mathbf{v}_{i\mathcal{B}} \end{bmatrix}, \quad \mathbf{A}_b^S \begin{bmatrix} \mathbf{v}_{i\mathcal{A}} \\ -\mathbf{v}_{i\mathcal{B}} \end{bmatrix} = \xi_i^b \begin{bmatrix} -\mathbf{v}_{i\mathcal{A}} \\ \mathbf{v}_{i\mathcal{B}} \end{bmatrix}. \quad (23)$$

Adding or subtracting these two equations gives

$$\mathbf{A}_b^S \begin{bmatrix} \mathbf{v}_{i\mathcal{A}} \\ \mathbf{0} \end{bmatrix} = \xi_i^b \begin{bmatrix} \mathbf{0} \\ \mathbf{v}_{i\mathcal{B}} \end{bmatrix}, \quad \mathbf{A}_b^S \begin{bmatrix} \mathbf{0} \\ -\mathbf{v}_{i\mathcal{B}} \end{bmatrix} = \xi_i^b \begin{bmatrix} \mathbf{v}_{i\mathcal{A}} \\ \mathbf{0} \end{bmatrix}, \quad (24)$$

which implies that $\mathbf{v}_{i\mathcal{A}} = \mathbf{0}$ if and only if $\mathbf{v}_{i\mathcal{B}} = \mathbf{0}$. Since $\|\mathbf{v}_{i\mathcal{A}}\|_2^2 + \|\mathbf{v}_{i\mathcal{B}}\|_2^2 = \|\mathbf{v}_i\|_2^2 = 1$, we conclude that $\mathbf{v}_{i\mathcal{A}}$ and $\mathbf{v}_{i\mathcal{B}}$ are both non-zero.

Now we turn to prove that $\mathbf{U}_b(\mathcal{A}, \mathcal{I}_r)$ has full column rank. For any $i < j \leq r \leq p$, since $\{\xi_i^b\}_{i=1}^N$ are in descending order, we have $\xi_i^b, \xi_j^b > 0$. Therefore, as discussed above, both $\mathbf{v}_{i\mathcal{A}}$ and $\mathbf{v}_{j\mathcal{A}}$ are non-zero vectors. Considering $\xi_i^b > 0$, we know that $-\xi_i^b < 0$ is also an eigenvalue of \mathbf{A}_b^S whose associated eigenvector is $\mathbf{v}_{-i} = [\mathbf{v}_{i\mathcal{A}}^\top, -\mathbf{v}_{i\mathcal{B}}^\top]^\top$. Thus,

$$\begin{aligned} \mathbf{v}_i^\top \mathbf{v}_j &= \mathbf{v}_{i\mathcal{A}}^\top \mathbf{v}_{j\mathcal{A}} + \mathbf{v}_{i\mathcal{B}}^\top \mathbf{v}_{j\mathcal{B}} = \mathbf{0}, \\ \mathbf{v}_{-i}^\top \mathbf{v}_j &= \mathbf{v}_{i\mathcal{A}}^\top \mathbf{v}_{j\mathcal{A}} - \mathbf{v}_{i\mathcal{B}}^\top \mathbf{v}_{j\mathcal{B}} = \mathbf{0}, \end{aligned} \quad (25)$$

which implies that $\mathbf{v}_{i\mathcal{A}}^\top \mathbf{v}_{j\mathcal{A}} = \mathbf{0}$. Consequently, $\mathbf{U}_b(\mathcal{A}, \mathcal{I}_r)$ has full column rank.

Similarly, we can show that $\mathbf{U}_b(\mathcal{B}, \mathcal{I}_s)$ also has full column rank. The invertibility of $\mathbf{I}_N + \mathbf{K}_b \mathbf{G}_b$ is a direct consequence of Theorem 2. ■

Proposition 3 shows that we can employ the commonly used sampling pattern when the graph is bipartite. Besides, other

sampling patterns can also be chosen as long as the conditions proposed in Proposition 3 are met. This is useful when the bipartite graph has an unbalanced partition of vertices, i.e. the sizes of the two parts $|\mathcal{A}|, |\mathcal{B}|$ differ a lot in which case the natural sampling pattern may lead to a low compression ratio (keep the larger part in LP channel) or a great loss of information (keep the smaller part in LP channel). Then we can search for other sampling patterns to produce a balanced partition that satisfy the conditions.

B. Formulating the Optimization Problems

By definition, \mathbf{G} is determined by the weights $\mathbf{w} \in \mathbb{R}^J$ when the graph is given. In order to obtain the desired filter responses, optimization models will be formulated to compute \mathbf{w} . For example, we can minimize $\|\mathbf{H}_L - \mathbf{H}^{\text{ideal}}\|_2$ to make \mathbf{H}_L approximate the ideal lowpass filter $\mathbf{H}^{\text{ideal}}$ whose response is given as:

$$\mathbf{h}^{\text{ideal}}(k) = \begin{cases} 1, & \xi_k \geq \xi_0, \\ 0, & \text{otherwise,} \end{cases}, \quad k = 1, \dots, N \quad (26)$$

where $\xi_0 \in [\xi_N, \xi_1]$ is a pre-determined threshold and $\{\xi_k\}_{k=1}^N$ are the eigenvalues of \mathbf{A}^S in descending order.

We will list the constraints of the optimization model to meet the conditions in Theorem 2. Without loss of generality, assume that the eigenvalues $\{\xi_i\}_{i=1}^N$ of \mathbf{A}^S are distinct. For a fixed $J \geq 2$, let $\mathbf{C} \in \mathbb{R}^{N \times J}$ be the Vandermonde matrix generated by $\{\xi_i\}_{i=1}^N$, i.e.,

$$\mathbf{C} = \begin{bmatrix} 1 & \xi_1 & \cdots & \xi_1^{J-1} \\ 1 & \xi_2 & \cdots & \xi_2^{J-1} \\ \vdots & \vdots & \ddots & \vdots \\ 1 & \xi_N & \cdots & \xi_N^{J-1} \end{bmatrix},$$

recall that $\mathbf{G} = \sum_{l=1}^J w_l (\mathbf{A}^S)^{l-1} = \mathbf{U} \mathbf{\Gamma} \mathbf{U}^\top$, then $\mathbf{\Gamma} = \text{diag}(\mathbf{C} \mathbf{w})$. Thus, the analysis filter responses are given as

$$\mathbf{h}_L = \frac{1}{2}(\mathbf{1} + \mathbf{C} \mathbf{w}), \quad \mathbf{h}_H = \frac{1}{2}(\mathbf{1} - \mathbf{C} \mathbf{w}). \quad (27)$$

Let $\mathbf{C}_r, \mathbf{C}_s$ and \mathbf{C}_m respectively denote the submatrices formed by the first r rows, the last s rows and the rest rows of \mathbf{C} . Consider the first set of conditions in Theorem 2:

$$\begin{aligned} \gamma_1 &= \cdots = \gamma_r = 1, \quad \gamma_{N+1-s} = \cdots = \gamma_N = -1, \\ \gamma_i &\in (-1, 1), \quad i = r+1, \dots, N-s, \end{aligned}$$

and construct such a convex optimization problem:

$$\begin{cases} \min_{\mathbf{w} \in \mathbb{R}^J} & \|\mathbf{h}^{\text{ideal}} - \frac{1}{2}(\mathbf{1} + \mathbf{C} \mathbf{w})\|_\infty \\ \text{s.t.} & \mathbf{C}_r \mathbf{w} = \mathbf{1}_r \\ & \mathbf{C}_s \mathbf{w} = -\mathbf{1}_s \\ & |\mathbf{C}_m \mathbf{w}| < \mathbf{1}_{N-r-s} \end{cases}. \quad (28)$$

Note that the objective function is actually equivalent to $\|\mathbf{H}^{\text{ideal}} - \mathbf{H}_L\|_2$.

When $r = s = 1$, the problem (28) is always feasible for any $J \geq 2$, since

$$\mathbf{w} = \left[-\frac{\xi_N + 1}{1 - \xi_N}, \frac{2}{1 - \xi_N}, 0, \dots, 0 \right] \in \mathbb{R}^J$$

is in the feasible domain (note that $\xi_1 = 1$). While in other cases, one should pay close attention to the feasibility of the problem since we cannot guarantee that the feasible domain is non-empty for all settings of r, s, J . Therefore, it is recommended to take $r = s = 1$ if you do not want to test the feasibility of the problem with r, s, J in other settings.

Recall that the spline-like filters are localized in the graph domain, and the smaller J is, the better the locality. However, low-order polynomials may not provide a good approximation of the ideal lowpass filter, as shown in the left of Figure 3, unexpected peaks and valleys may appear in the middle section of the polynomial filter response. For this rationale, we would like to add a regularization term $R(\mathbf{h}_L)$ to the original objective function to improve the smoothness of \mathbf{h}_L . Denote p_L the polynomial associated with \mathbf{h}_L , i.e.,

$$p_L(x) = 1 + \sum_{l=1}^J w_l x^{l-1}, \quad x \in [\xi_N, \xi_1].$$

Consider the 2-norm of function p_L :

$$\|p_L\|_2 = \int_{\xi_N}^{\xi_1} |p'_L(x)|^2 dx = \int_{\xi_N}^{\xi_1} \left| \sum_{l=1}^{J-1} w_{l+1} l x^{l-1} \right|^2 dx. \quad (29)$$

Let $R(\mathbf{h}_L)$ be the discrete version:

$$R(\mathbf{h}_L) = \sum_{i=1}^N |p'_L(\xi_i)|^2 = \|\mathbf{C}_0 \text{diag}(0, \dots, J-1) \mathbf{w}\|_2, \quad (30)$$

where

$$\mathbf{C}_0 = \begin{bmatrix} 0 & 1 & \xi_1 & \cdots & \xi_1^{J-2} \\ 0 & 1 & \xi_2 & \cdots & \xi_2^{J-2} \\ \vdots & \vdots & \vdots & \ddots & \vdots \\ 0 & 1 & \xi_N & \cdots & \xi_N^{J-2} \end{bmatrix} \in \mathbb{R}^{N \times J}.$$

Then, the regularized optimization problem is

$$\begin{cases} \min_{\mathbf{w} \in \mathbb{R}^J} & \|\mathbf{h}^{\text{ideal}} - \frac{1}{2}(\mathbf{1} + \mathbf{C}\mathbf{w})\|_\infty + \alpha R(\mathbf{h}_L) \\ \text{s.t.} & \mathbf{C}_r \mathbf{w} = \mathbf{1}_r \\ & \mathbf{C}_s \mathbf{w} = -\mathbf{1}_s \\ & |\mathbf{C}_m \mathbf{w}| < \mathbf{1}_{N-r-s} \end{cases}, \quad (31)$$

where $\alpha \geq 0$ is a parameter that controls the importance of the regularization term.

For simplicity, we refer to the proposed two optimization models (28) and (31) as **oriOpt** and **regOpt** respectively, and the model (8) proposed in [7] as **literOpt**. Figure 3 shows an example of the lowpass filter responses determined by these three models, where the parameters are taken to be $(r, s, J, \alpha) = (2, 3, 8, 0.5)$, and the desired filter responses are all $\mathbf{h}^{\text{ideal}}$. In this work, we always use CVX, a package for specifying and solving convex programs [10], [9], to solve the optimization problems.

It is shown that regularized method outperforms the other two methods. As we have expected, oriOpt produces an oscillatory solution, which is less ideal than the smooth solution produced by regOpt. It is worth mentioning that for literOpt, we have done a lot of experiments with various values of J on a lot of random sensor graphs, it always gave a linear filter response.

C. Determining the Partition $\{\mathcal{A}, \mathcal{B}\}$

According to Theorem 2, the sampling matrix \mathbf{K} is determined by the partition $\{\mathcal{A}, \mathcal{B}\}$ of \mathcal{V} . Given a normalized adjacency matrix \mathbf{A}^S , Algorithm 1 outputs a partition $\{\mathcal{A}, \mathcal{B}\}$ of \mathcal{V} that makes the matrices $\mathbf{U}(\mathcal{A}, \mathcal{I}_r)$ and $\mathbf{U}(\mathcal{B}, \mathcal{I}_s)$ have full column rank. The symbol “ \ll ” means “much smaller than”, and the operation $\mathcal{V} \setminus \mathcal{A}$ computes the difference between two sets.

Algorithm 1 Search for $\{\mathcal{A}, \mathcal{B}\}$

Input: Normalized adjacency matrix \mathbf{A}^S , $1 \leq r, s \ll N$

- 1: Initialization: Set $\mathcal{V} = \{1, \dots, N\}$, $\mathcal{A} = \emptyset, \mathcal{B} = \emptyset$, $\mathbf{U}_r = \mathbf{U}(\mathcal{V}, \mathcal{I}_r)$, $\mathbf{U}_s = \mathbf{U}(\mathcal{V}, \mathcal{I}_s)$
- 2: Compute the row echelon form of \mathbf{U}_r to obtain r linearly independent rows, and add their indices to \mathcal{A}
- 3: **if** $\mathbf{U}_s(\mathcal{V} \setminus \mathcal{A}, \mathcal{I}_s)$ is not full column rank **then**
- 4: Throw an error, quit and reset r and s
- 5: **else**
- 6: Compute the row echelon form of $\mathbf{U}_s(\mathcal{V} \setminus \mathcal{A}, \mathcal{I}_s)$ to obtain s linearly independent rows, and add their indices to \mathcal{B}
- 7: Partition the rest row indices into two balanced sets based on some criterion, and assign them to \mathcal{A} and \mathcal{B} respectively

8: **end if**

Output: \mathcal{A}, \mathcal{B}

Next, we discuss how the partition $\{\mathcal{A}, \mathcal{B}\}$ will affect the approximation error of the filterbank. Let \mathbf{K} be the sampling matrix defined by (14). If we only use the LP output \mathbf{y}_L of the analysis stage for reconstruction, the reconstructed signal would be $\mathbf{y}' = \frac{1}{2} \mathbf{H}_{\text{INV}}(\mathbf{I}_N + \mathbf{K})\mathbf{y}_L$. Thus, the approximation error of \mathbf{y}' to the original signal is $\|\mathbf{x} - \mathbf{y}'\|_2$. Since the filterbank is perfectly reconstructed, there holds $\mathbf{y} = \mathbf{x}$, where \mathbf{y} is the total reconstruction defined by (1). Consequently, the approximation error of the filterbank is defined as

$$\begin{aligned} \text{er} &= \|\mathbf{y} - \mathbf{y}'\|_2 \\ &= \left\| \frac{1}{4} \mathbf{H}_{\text{INV}}(\mathbf{I}_N - \mathbf{K})(\mathbf{I}_N - \mathbf{G})\mathbf{x} \right\|_2 \\ &\leq \frac{1}{4} \|\mathbf{H}_{\text{INV}}\|_2 \|(\mathbf{I}_N - \mathbf{K})\|_2 \|(\mathbf{I}_N - \mathbf{G})\|_2 \|\mathbf{x}\|_2 \\ &= 2 \|(\mathbf{I}_N + \mathbf{K}\mathbf{G})^{-1}\|_2 \|\mathbf{x}\|_2 \\ &= \frac{2}{\sigma_{\min}(\mathbf{I}_N + \mathbf{K}\mathbf{G})} \|\mathbf{x}\|_2, \end{aligned} \quad (32)$$

where σ_{\min} represents the smallest singular value of a matrix. Here we exploit the facts that $\mathbf{H}_{\text{INV}} = 2(\mathbf{I}_N + \mathbf{K}\mathbf{G})^{-1}$ and $\|(\mathbf{I}_N - \mathbf{K})\|_2 = \|(\mathbf{I}_N - \mathbf{G})\|_2 = 2$. Although $\sigma_{\min}(\mathbf{I}_N + \mathbf{K}\mathbf{G}) \neq 0$ can be guaranteed by Theorem 2, a small value may also lead to poor approximation. Considering that r, s are usually set to be small, the method of partitioning the rest vertices in Step 7 of Algorithm 1 is the major factor affecting the value of $\sigma_{\min}(\mathbf{I}_N + \mathbf{K}\mathbf{G})$.

We conduct experiments to compare two strategies. One is to partition the rest vertices according to the polarity of entries of \mathbf{u}_N [23]: if $\mathbf{u}_N(i) < 0$ then i is added to \mathcal{B} ; otherwise it is added to \mathcal{A} . Another strategy is a random method which

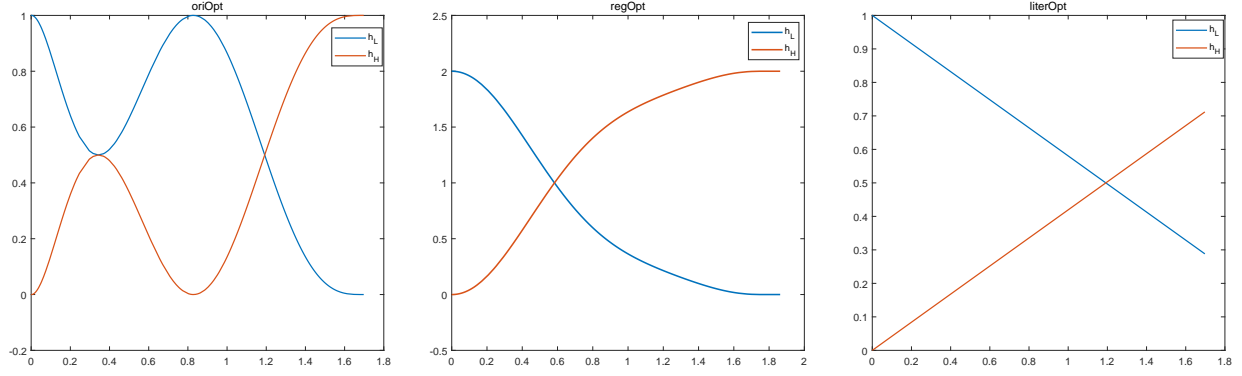


Fig. 3. From left to right are the filter responses produced respectively by the three optimization models: oriOpt, regOpt and literOpt, blue for lowpass and red for highpass. The horizontal axis represents the eigenvalues of \mathbf{L}^S , in which the duplicate eigenvalues have been removed before solving the optimization problems.

randomly partitions the rest vertices into two balanced sets \mathcal{A} and \mathcal{B} . Other strategies can also be employed as needed.

Experiments are performed on 100 randomly generated bipartite graphs and 100 random sensor graphs respectively. All graphs have 100 vertices, and each bipartite graph has two parts of size (20, 80). We solve the regOpt with $(r, s, J, \alpha) = (1, 1, 3, 0.5)$ to obtain the weights \mathbf{w} and thus \mathbf{G} . Figure 4 and Figure 5 show the smallest singular values $\sigma_{\min}(\mathbf{I}_N + \mathbf{K}\mathbf{G})$ using the first strategy and the second strategy respectively. It shows that the first one is better. In fact, a random strategy is not reasonable, because we need to reconnect the down-sampled vertices to obtain a new graph for multi-resolution analysis. Therefore, we want the vertices within each set of $\{\mathcal{A}, \mathcal{B}\}$ to be connected by edges with low weights. The first strategy performs better because it is closely related to the nodal domain theory. For more details, please refer to [1], [23]. Besides, other methods such as k -means clustering on \mathbf{u}_N [23], or solving the max-cut problem to obtain the partition can also be used [19].

Figure 6 shows the approximation errors of the proposed filterbanks on 10 random sensor graphs. For each graph, we synthesize 100 signals, each with unit norm. Only the LP output is used for reconstruction and the approximation error is computed according to the definition (32). We solve the regOpt with $(r, s, J, \alpha) = (1, 1, 3, 0.5)$. The upper bounds $\frac{2}{\sigma_{\min}(\mathbf{I}_N + \mathbf{K}\mathbf{G})}$ associated with each graph are also calculated, all of which are in the order of thousands, much greater than the approximation errors in the experiment.

D. Annihilating the DC Signal

In applications where the intrinsic graphs are located in the physical space, a constant signal (called DC signal) may have a physical interpretation, and the highpass filter should be able to annihilate the DC signal. However, the spline-like filterbanks proposed in Section III-A are based on the normalized adjacency matrix \mathbf{A}^S . Thus, the highpass filter $\mathbf{H}_H = \frac{1}{2}(\mathbf{I}_N - \mathbf{G})$ has a zero response to \mathbf{u}_1 , the eigenvector of \mathbf{L}^S associated with $\lambda_1 = 0$, which is not a constant vector unless \mathcal{G} is a regular graph (i.e., all vertices have the same

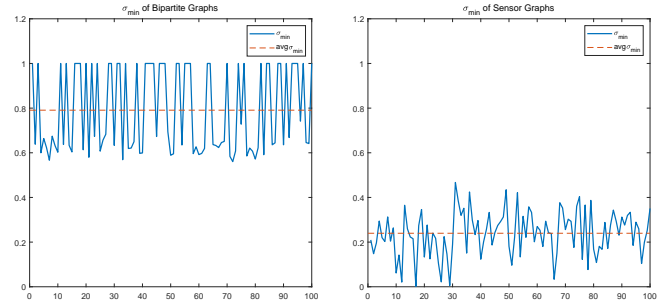


Fig. 4. The smallest singular values $\sigma_{\min}(\mathbf{I}_N + \mathbf{K}\mathbf{G})$ on random graphs using the first strategy and their average $\text{avg}\sigma_{\min}$. Left: σ_{\min} of random bipartite graphs; Right: σ_{\min} of random sensor graphs.

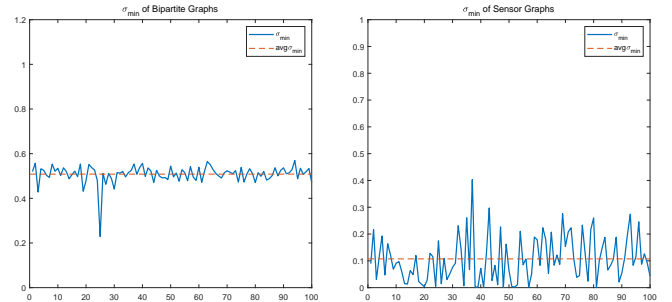


Fig. 5. The smallest singular values $\sigma_{\min}(\mathbf{I}_N + \mathbf{K}\mathbf{G})$ on random graphs using the second strategy.

degree). In this case, filtering the DC signal with \mathbf{H}_H may produce a non-zero result. Since $\mathbf{u}_1 = \mathbf{D}^{1/2}\mathbf{1}$, this problem can be addressed by pre-multiplying the input signal \mathbf{x} with $\mathbf{D}^{1/2}$, and post-multiplying the filtered signal with $\mathbf{D}^{-1/2}$ [18]. Define the zero-DC analysis filters as:

$$\begin{cases} \mathbf{H}_L^0 = \mathbf{D}^{-1/2}\mathbf{H}_L\mathbf{D}^{1/2} \\ \mathbf{H}_H^0 = \mathbf{D}^{-1/2}\mathbf{H}_H\mathbf{D}^{1/2} \end{cases} \quad (33)$$

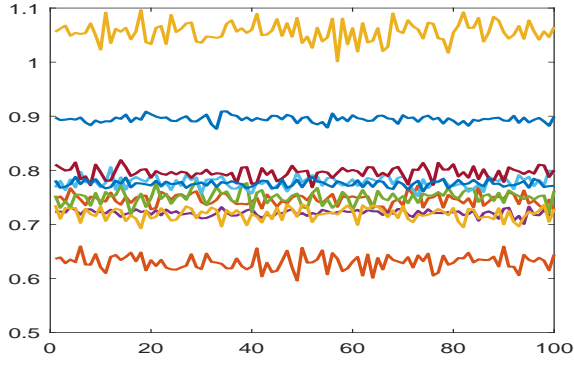


Fig. 6. The approximation errors of the proposed filterbanks on 10 random sensor graphs. Each line represents the approximation errors resulting from the decomposition of 100 signals on a graph.

Then the whole transform of the filterbank becomes

$$\begin{aligned}
 \mathbf{y} &= \mathbf{H}_{\text{INV}}^0 \left[\frac{1}{2}(\mathbf{I}_N + \mathbf{K})\mathbf{H}_L^0 + \frac{1}{2}(\mathbf{I}_N - \mathbf{K})\mathbf{H}_H^0 \right] \mathbf{x} \\
 &= \mathbf{H}_{\text{INV}}^0 \left[\frac{1}{2}(\mathbf{I}_N + \mathbf{K})\mathbf{D}^{-1/2}\mathbf{H}_L\mathbf{D}^{1/2} \right. \\
 &\quad \left. + \frac{1}{2}(\mathbf{I}_N - \mathbf{K})\mathbf{D}^{-1/2}\mathbf{H}_H\mathbf{D}^{1/2} \right] \mathbf{x} \\
 &= \mathbf{H}_{\text{INV}}^0 \left[\frac{1}{2}(\mathbf{I}_N + \mathbf{K}\mathbf{D}^{-1/2}\mathbf{G}\mathbf{D}^{1/2}) \right] \mathbf{x},
 \end{aligned} \tag{34}$$

where $\mathbf{H}_{\text{INV}}^0$ represents the synthesis filter. Since \mathbf{D} and \mathbf{K} are commutative, $\mathbf{I}_N + \mathbf{K}\mathbf{D}^{-1/2}\mathbf{G}\mathbf{D}^{1/2}$ is invertible iff $\mathbf{I}_N + \mathbf{K}\mathbf{G}$ is invertible. Therefore, as long as \mathbf{K} and \mathbf{G} satisfy the conditions proposed in Theorem 2, the synthesis filter exists and is given as

$$\mathbf{H}_{\text{INV}}^0 = 2\mathbf{D}^{-1/2}(\mathbf{I}_N + \mathbf{K}\mathbf{G})^{-1}\mathbf{D}^{1/2}. \tag{35}$$

IV. EXPERIMENTS

In this section, we will evaluate the performance of the proposed filterbanks and compare them with related works. All experiments are done with Matlab and the GSP toolbox [21].

First, we specify the hyperparameters (r, s, J, α) and solve the optimization problems to obtain the weights \mathbf{w} and thus \mathbf{G} . Second, implement Algorithm 1 to compute a partition \mathcal{A}, \mathcal{B} according to the polarity of the entries of \mathbf{u}_N , then construct the sampling matrix \mathbf{K} by (14). We will employ the zero-DC filters $\mathbf{H}_L^0, \mathbf{H}_H^0, \mathbf{H}_{\text{INV}}^0$ defined in Section III-D to form the proposed filterbanks. Multi-resolution analysis will be performed on the graph signals, thus, after downsampling, the Kron reduction scheme [6] is used to reconnect the vertices in \mathcal{A} to produce a reduced graph, further decomposition will be recursively performed on the lowpass channel.

A. Locality of the Proposed Filterbanks

We use GSP toolbox to generate a bipartite ring graph with $N = 512$ vertices. The corresponding graph signal \mathbf{x} is piecewise constant, i.e., the first half of \mathbf{x} are all ones, and the second half are all zeros, as shown in the left top of Figure 7. We solve the regOpt (31) with $(r, s, J, \alpha) = (1, 1, 4, 1)$.

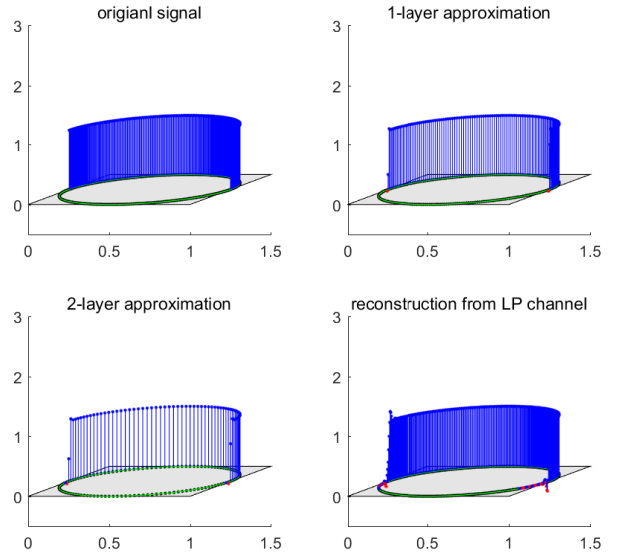


Fig. 7. Multi-resolution analysis of the graph signal located on a bipartite ring graph. Left Top: the original signal; Right Top: the LP output in the 1st layer; Left Bottom: the LP output in the 2nd layer; Right Bottom: the reconstructed signal using only the LP output from the 2nd layer decomposition.

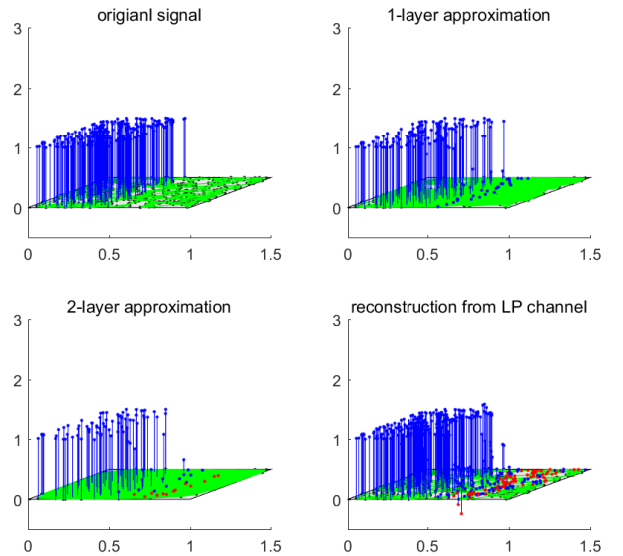


Fig. 8. Multi-resolution analysis of the graph signal located on a sensor graph. Left Top: the original signal; Right Top: the LP output in the 1st layer; Left Bottom: the LP output in the 2nd layer; Right Bottom: the reconstructed signal using only the LP output from the 2nd layer decomposition.

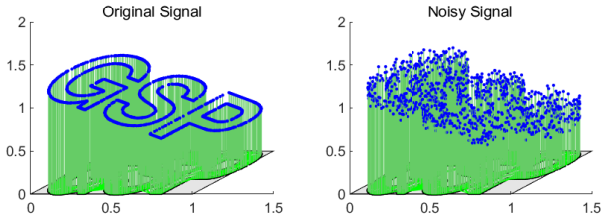


Fig. 9. Left: the original signal; Right: the noisy signal.

Figure 7 shows the LP outputs in each layer decomposition and the reconstructed signal using only the LP output of the last layer. It can be seen that there is no significant Gibbs effect near the discontinuity points of the LP outputs, indicating that the analysis filters are well localized in the graph domain.

We also compute the relative error of each LP output and the reconstructed signal. Let y_i be the LP output of i -th layer and x_i be the corresponding ideal output, i.e., x_i is a subvector of x whose element indices are in the downsampled subset \mathcal{A} of i -th layer. The relative error of y_i with respect to (w.r.t.) x_i is defined as $e_i = \frac{\|y_i - x_i\|_2}{\|x_i\|_2}$. Let y be the reconstructed signal, then the relative error of y w.r.t. x is $e = \frac{\|y - x\|_2}{\|x\|_2}$. In the experiment, we get

$$e_1 = 0.032, \quad e_2 = 0.067, \quad e = 0.063.$$

Besides, the same experiment is conducted on a random sensor graph with 512 vertices, which is not bipartite. The results are shown in Figure 8 and the relative errors are

$$e_1 = 0.057, \quad e_2 = 0.081, \quad e = 0.166.$$

B. Comparison with Related Work

In this section, we perform MRA on graph signals to compare the proposed model with related works in terms of approximation ability of the coarsened signals and denoising ability. The related schemes are literOpt [7] and two other state-of-the-art spline-like graph filterbanks: MSGFB [16] and SGFBSS [17]. MSGFB is an improved model of literOpt which relaxes the constraints of the optimization problem (8) for better solution. Unlike regOpt, literOpt and MSGFB, which sample in the vertex domain, SGFBSS adopts the spectral domain sampling method proposed in [25].

1) *Approximation*: We generate the gspLogo graph with $N = 1130$ and synthesize a signal x^0 which is a linear function of the x -coordinates of the vertices. Then x^0 is contaminated with Gaussian noise of zero mean and $1/16$ standard deviation to produce a noisy signal x , as shown in Figure 9. A 1-layer decomposition is performed on the graph signal, where the hyperparameters are specified as $(r, s, J, \alpha) = (1, 4, 5, 0.01)$ for regOpt (31) and $J = 5$ for literOpt, MSGFB and SGFBSS.

In each layer decomposition of MRA, the LP output and the corresponding reduced graph serve as a coarser approximation of the original signal and graph. Figure 10 depicts the LP output of each model. It can be seen that the proposed filterbank outperforms the others. We also compute the corresponding relative errors. Let y_i and x_i have the same definitions as

in Section IV-A. Then the relative errors of y_i w.r.t. x_i are 0.02, 0.04, 0.5, 1.67 for regOpt, literOpt, MSGFB and SGFBSS, respectively.

To be mentioned, the model SGFBSS cannot preserve signal values in the vertex domain due to the spectral sampling scheme, which makes the LP output differ a lot from the original signal, as shown in the right bottom image of Figure 10.

2) *Denoising*: Next, let us compare the denoising ability of the proposed method regOpt with the related methods. Experiments are performed on the ring graph with 64 vertices, the Comet graph with 64 vertices and the gspLogo graph with 1130 vertices. The synthetic graph signals x are presented respectively in the vertex domain and the spectral domain in Figure 11. We contaminate the signals with Gaussian noise of zero mean and different standard deviations $\sigma = 1/16, 1/8, 1/4$. In the experiment, all the LP outputs are retained and HP outputs are hard-thresholded with the value $T = 3\sigma$ for reconstruction.

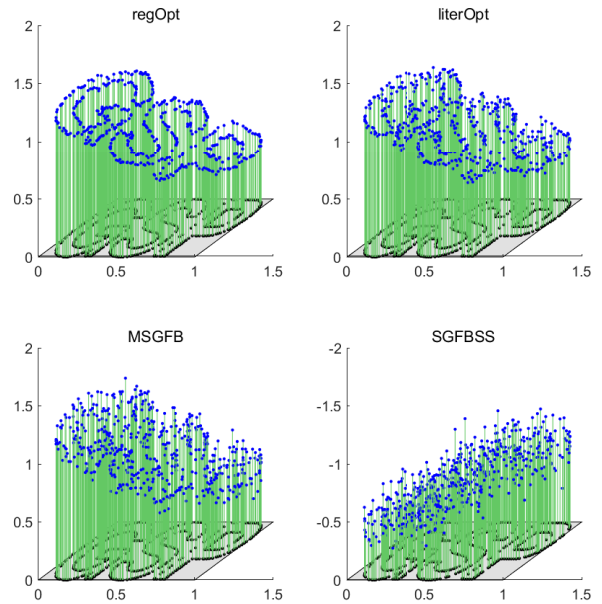


Fig. 10. The LP outputs of each model.

We perform a 2-layer decomposition for the ring graph and the Comet graph, and a 1-layer decomposition for the gspLogo graph because SGFBSS requires N to be even and there are 565 vertices in the 2nd layer. The hyperparameters are specified as $(r, s, J, \alpha) = (2, 3, 6, 0.01)$ for regOpt and $J = 6$ for the other models. The relative error $\frac{\|y - x\|_2}{\|x\|_2}$ between the original signal x and the reconstructed signal y is computed, as shown in Figure 12. The results show that the proposed model regOpt outperforms the other models in most cases.

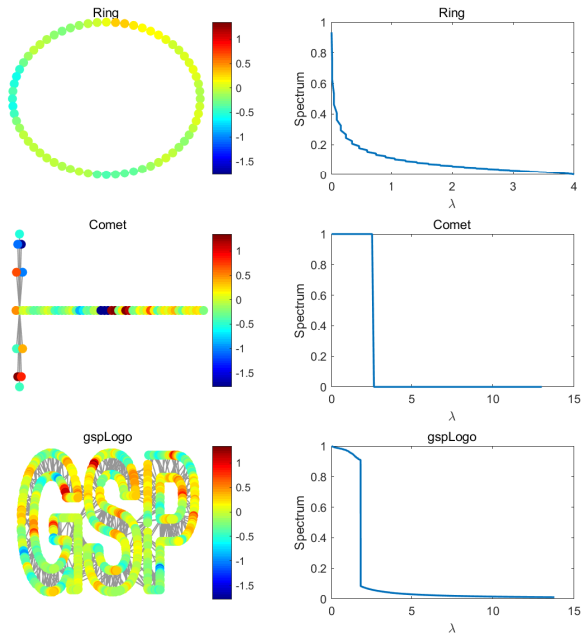


Fig. 11. The synthetic graph signals in the vertex domain and the spectral domain.

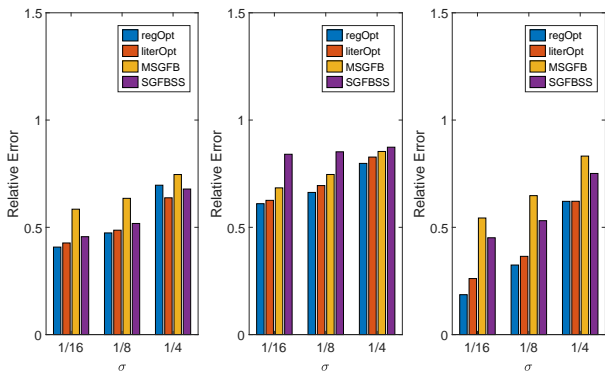


Fig. 12. The average relative errors of 10 runs using different models. Left: Ring graph; Middle: Comet graph; Right: gspLogo graph.

V. CONCLUSION AND FUTURE WORK

This paper describes a class of critically sampled and perfectly reconstructed spline-like filterbanks for graph signals. The analysis filters are polynomials in the normalized adjacency matrix, which allows the performance of local analysis in the vertex domain. Besides, the lowpass filters can remove the s highest frequency components of the signals, and the highpass filters can remove the r lowest frequency components of the signals, where r and s are hyperparameters specified by the users. When $r, s \geq 1$, the proposed filterbanks will outperform the filterbanks proposed in the related work on denoising tasks.

The main limitation of the proposed filterbank is that the synthesis filter is usually not well localized. It can be challenging but rewarding to design localized synthesis filters in future work. We also mentioned that the approximation error of the filterbank is bounded by the multiple of the largest

singular value of $(\mathbf{I}_N + \mathbf{K}\mathbf{G})^{-1}$. Empirically, we adopt a sampling pattern that prevents the smallest singular value of $\mathbf{I}_N + \mathbf{K}\mathbf{G}$ from being too small, but it may occasionally fail. In fact, this upper bound is too loose to effectively reflect the approximation error of the filterbank. As presented in the experiments on random graphs and random signals, the largest singular value of $(\mathbf{I}_N + \mathbf{K}\mathbf{G})^{-1}$ is always much greater than the approximation errors. Thus, the future research should consider finding a tighter upper bound.

REFERENCES

- [1] Türker Biyikoglu, Josef Leydold, and Peter F Stadler. *Laplacian eigenvectors of graphs: Perron-Frobenius and Faber-Krahn type theorems*. Springer, 2007.
- [2] Fan RK Chung. Lectures on spectral graph theory. *CBMS Lectures, Fresno*, 6(92):17–21, 1996.
- [3] Fan RK Chung and Fan Chung Graham. *Spectral graph theory*, volume 92. American Mathematical Soc., 1997.
- [4] Ronald R Coifman and Mauro Maggioni. Diffusion wavelets. *Applied and Computational Harmonic Analysis*, 21(1):53–94, 2006.
- [5] Mark Crovella and Eric Kolaczyk. Graph wavelets for spatial traffic analysis. In *IEEE INFOCOM 2003. Twenty-second Annual Joint Conference of the IEEE Computer and Communications Societies (IEEE Cat. No. 03CH37428)*, volume 3, pages 1848–1857. IEEE, 2003.
- [6] Florian Dorfler and Francesco Bullo. Kron reduction of graphs with applications to electrical networks. *IEEE Transactions on Circuits and Systems I: Regular Papers*, 60(1):150–163, 2013.
- [7] Venkatesan N. Ekambaram, Giulia C. Fanti, Babak Ayazifar, and Kannan Ramchandran. Spline-like wavelet filterbanks for multiresolution analysis of graph-structured data. *IEEE Transactions on Signal and Information Processing Over Networks*, 1(4):268–278, 2015.
- [8] Matan Gavish, Boaz Nadler, and Ronald R Coifman. Multiscale wavelets on trees, graphs and high dimensional data: Theory and applications to semi supervised learning. In *ICML*, 2010.
- [9] Michael Grant and Stephen Boyd. Graph implementations for nonsmooth convex programs. In V. Blondel, S. Boyd, and H. Kimura, editors, *Recent Advances in Learning and Control*, Lecture Notes in Control and Information Sciences, pages 95–110. Springer-Verlag Limited, 2008. http://stanford.edu/~boyd/graph_dcp.html.
- [10] Michael Grant and Stephen Boyd. CVX: Matlab software for disciplined convex programming, version 2.1. <http://cvxr.com/cvx>, March 2014.
- [11] David K Hammond, Pierre Vandergheynst, and Rémi Gribonval. Wavelets on graphs via spectral graph theory. *Applied and Computational Harmonic Analysis*, 30(2):129–150, 2011.
- [12] Qianjiang Hu, Daizong Liu, and Wei Hu. Exploring the devil in graph spectral domain for 3d point cloud attacks. In *Computer Vision—ECCV 2022: 17th European Conference, Tel Aviv, Israel, October 23–27, 2022, Proceedings, Part III*, pages 229–248. Springer, 2022.
- [13] M. S Kotzagiannidis and P. L Dragotti. Splines and wavelets on circulant graphs. *Applied and Computational Harmonic Analysis*, page S1063520317301215, 2016.
- [14] Daizong Liu, Wei Hu, and Xin Li. Point cloud attacks in graph spectral domain: When 3d geometry meets graph signal processing. *arXiv preprint arXiv:2207.13326*, 2022.
- [15] Daizong Liu, Shuangjie Xu, Xiao-Yang Liu, Zichuan Xu, Wei Wei, and Pan Zhou. Spatiotemporal graph neural network based mask reconstruction for video object segmentation. In *Proceedings of the AAAI Conference on Artificial Intelligence*, volume 35, pages 2100–2108, 2021.
- [16] Amir Miraki and Hamid Saeedi-Sourck. A modified spline graph filter bank. *Circuits, Systems, and Signal Processing*, 40:2025–2035, 2021.
- [17] Amir Miraki and Hamid Saeedi-Sourck. Spline graph filter bank with spectral sampling. *Circuits, Systems, and Signal Processing*, 40(11):5744–5758, 2021.
- [18] Narang, S.K, Ortega, and A. Compact support biorthogonal wavelet filterbanks for arbitrary undirected graphs. *IEEE Transactions on Signal Processing*, 61(19):4673–4685, 2013.
- [19] S. K. Narang and A. Ortega. Local two-channel critically sampled filter-banks on graphs. In *IEEE International Conference on Image Processing*, 2010.
- [20] Sunil K Narang and Antonio Ortega. Perfect reconstruction two-channel wavelet filter banks for graph structured data. *IEEE Transactions on Signal Processing*, 60(6):2786–2799, 2012.

- [21] Nathanaël Perraudin, Johan Paratte, David Shuman, Lionel Martin, Vassilis Kalofolias, Pierre Vandergheynst, and David K. Hammond. GSPBOX: A toolbox for signal processing on graphs. *ArXiv e-prints*, August 2014.
- [22] A. Sandryhaila and J. M. F. Moura. Discrete signal processing on graphs: Graph Fourier transform. In *2013 IEEE International Conference on Acoustics, Speech and Signal Processing*, pages 6167–6170, Vancouver, BC, Canada, 2013.
- [23] D. I. Shuman, M. J. Faraji, and P. Vandergheynst. A multiscale pyramid transform for graph signals. *IEEE Transactions on Signal Processing*, 64(8):2119–2134, 2016.
- [24] David I Shuman, Sunil K Narang, Pascal Frossard, Antonio Ortega, and Pierre Vandergheynst. The emerging field of signal processing on graphs: Extending high-dimensional data analysis to networks and other irregular domains. *IEEE signal processing magazine*, 30(3):83–98, 2013.
- [25] Yuichi Tanaka. Spectral domain sampling of graph signals. *IEEE Transactions on Signal Processing*, 66(14):3752–3767, 2018.
- [26] David BH Tay, Yuichi Tanaka, and Akie Sakiyama. Almost tight spectral graph wavelets with polynomial filters. *IEEE Journal of Selected Topics in Signal Processing*, 11(6):812–824, 2017.
- [27] Lihua Yang, Anna Qi, Chao Huang, and Jianfeng Huang. Graph Fourier transform based on ℓ_1 norm variation minimization. *Applied and Computational Harmonic Analysis*, 52:348–365, 2021.